Journal of Alloys and Compounds 774 (2019) 573–580

Contents lists available at ScienceDirect

Journal of Alloys and Compounds

journal homepage: http://www.elsevier.com/locate/jalcom

Microstructure evolution of as-cast AlN/AZ91 composites and room temperature compressive properties

Changlin Yang*, Bin Zhang, Dongchen Zhao, Xiaobo Wang, Yunxia Sun, Xinyue Xu,
Feng Liu**

State Key Laboratory of Solidification Processing, Northwestern Polytechnical University, Xi'an, Shaanxi, 710072, PR China

A R T I C L E I N F O

Article history:
Received 25 July 2018
Received in revised form
1 October 2018
Accepted 6 October 2018
Available online 8 October 2018

Keywords:
Magnesium matrix composites
Microstructure evolution
In-situ AlN particle
Compression strength
Compression ductility

A B S T R A C T

The microstructures of as-cast AlN/AZ91 composites prepared by different in-situ nitridation reaction times are characterized. Increasing nitridation reaction times resulted in morphological changes of the primary α-Mg phase from coarse dendritic structures to fine cellular structures, the volume fraction decrease of eutectic β-$Mg_{17}Al_{12}$ phase, and the eutectic structure transformation from partial divorced eutectic to fully divorced eutectic. During the room temperature compression of as-cast AlN/AZ91 composites, the (0002) basal plane texture perpendicular to the compression direction was weakened effectively, and compression strength and plasticity were simultaneously improved compared with as-cast AZ91 alloy. When the nitridation reaction time is 2 h, i.e. the volume fraction of in-situ AlN particles is 1.5%, the compressive yield strength of 110 ± 2 MPa, the ultimate compressive strength of 371 ± 8 MPa and the compressive fraction elongation of 22.1 ± 0.4% are achieved in the in-situ AlN/AZ91 composites.

© 2018 Elsevier B.V. All rights reserved.

1. Introduction

Magnesium matrix composites have shown great potential for aerospace and automotive industry due to low density, high specific strength and specific stiffness, good wear resistance and excellent casting performance [1]. Due to low manufacture costs and isotropic properties, ceramic particles are usually introduced into the matrix alloy as the reinforcement through the ex-situ synthetic techniques (stir casting, squeeze casting and powder metallurgy) and the in-situ synthetic techniques [2–7]. Although the ex-situ synthetic can easily introduce various scale ceramic particles into the magnesium matrix, a series of drawbacks, such as weak interface bonding, and more pores, etc., will be brought into the matrix alloys, which can result in a sharp deterioration of the plasticity [8–10]. In contrast, the in-situ synthetic technique not only can form nano-sized ceramic particles, but also the homogeneous distributions and strong bonding interface of the ceramic particles can be achieved. So in the present work, by the in-situ synthetic technique, the higher as-cast tensile strength (220–240 MPa) and fracture elongation (20–47%) were simultaneously obtained in the in-situ AlN particle reinforced Mg-9Al and AZ91 alloys [11–13].

In the previous work, only the compression strength can be improved in the ex-situ synthetized particle reinforced Mg matrix composites, while the compression ductility is decreased. However, the compression behaviors of the in-situ particle reinforced Mg matrix composites are not still clear. Especially, for the in-situ AlN/AZ91composites with higher tensile strength and fracture elongation in the present work, so it is necessary and interesting to investigate the compression behaviors to further extend the application fields.

Then, in the present paper, the compression behaviors of in-situ AlN/AZ91 composites prepared by a nitridation reaction between AZ91 matrix and N_2 are investigated, and the microstructure evolutions with the different amount of AlN particles and the compression deformation mechanism are also discussed, while the nitridation reaction mechanism between AZ91 matrix and N_2 was in detail described and discussed in Refs. [11–13]. In addition, considering that the nitridation reaction time is more available and controllable, while the nitridation reaction time is corresponding to the different volume fractions of in-situ AlN particles, herein, the nitridation reaction time was used to represent the different volume fractions of in-situ AlN particles.

2. Experimental

In this work, commercial AZ91 alloy was chosen as the matrix

---

* Corresponding author.
** Corresponding author.
E-mail addresses: ycl@nwpu.edu.cn (C. Yang), liufeng@nwpu.edu.cn (F. Liu).

https://doi.org/10.1016/j.jallcom.2018.10.041
0925-8388/© 2018 Elsevier B.V. All rights reserved.

alloy. Table 1 shows the chemical composition of AZ91 alloy (Magontec Xi'an Co., Ltd). Nitrogen gas with high purity (99.999%) was used as the reaction gas, and argon gas with high purity (99.999%) was used to maintain an inert atmosphere in the reaction chamber. Firstly, AZ91 alloy of 1300 g was placed in a vacuum resistance furnace. Before melting alloy, the chamber was vacuumed to 0.01 MPa firstly, and then backfilled with high purity argon gas to 0.1 MPa for several times. In the subsequent heating and cooling process, argon gas was kept at a certain flux (200 ml/min) to maintain an inert atmosphere in the reaction chamber. The temperature of the melt was monitored by a thermocouple positioned at the bottom of the crucible. When the temperature of the melt was 760 °C, a stainless steel tube with 18 nozzles of a diameter of 3 mm around the bottom was submerged into the melt near the bottom of the crucible, and then nitrogen gas was bubbled into the alloy melt for different times (0, 1, 1.5, 2, 2.5 h), respectively. During the nitridation reaction, the mechanical stirring was carried out to disperse the in-situ AlN ceramic particles uniformly. The flow rate and pressure of the nitrogen gas was kept at 420 ml/min and 0.4 MPa in the reaction process, respectively. After nitridation reaction, the alloy melt was held at the reactive temperature for 30 minutes. Lastly, the melt was poured into the permanent mould with a diameter of 20 mm.

The cylinder specimens with dimensions of Φ 10 mm × 15 mm were cut and machined from the mid-section of the castings to perform the compression tests. Uniaxial compression tests at room temperature of in-situ AlN/AZ91 composites were performed using the Instron 3382 Tester with a strain rate of $1 \times 10^{-3}\ s^{-1}$. The phases and X-ray pole figure of compression specimens of in-situ AlN/AZ91 composites were characterized and measured using a X-ray diffraction (Bruker D8 Discover) with Co $K_{\alpha 1}$ radiation ($\lambda = 1.7902$ Å), the range of diffraction angles (30°~130°) and scanning time (60s) at 35 kV and 40 mA current strength. The texture after compression tests was analyzed by measuring the intensity change of peaks along the transverse and longitudinal section of compression specimens. The pole figures were calculated using the quantitative texture analysis software MULTEX 3. The compression specimens were mechanically ground, subsequently polished and etched using a solution consisting of 3 vol% HNO_3 and 97 vol% C_2H_5OH at the room temperature for 12 s. Optical microscopy (OM), high resolution scanning electron microscopy (HRSEM, FEI Nova 450 SEM), field emission scanning electron microscopy (FESEM, Tescan MIRA 3 XMU) equipped with an energy dispersive spectrum (EDS) were employed to observe the microstructure and fracture surfaces after the compression tests. The particle interfaces during compressing were analyzed using transmission electron microscopy (TEM, JEM-2100). TEM specimens were cut parallel to the compression direction. TEM foils were prepared by a precision ion polishing system (Gatan 691, USA).

3. Results and discussion

3.1. The as-cast microstructure evolutions with different nitridation reaction times

Fig. 1 shows the XRD results of in-situ AlN/AZ91 composites with different nitridation reaction times, in which the AZ91 matrix alloy is composed of $Mg_{17}Al_{12}$ and α-Mg (Fig. 1a), and with increasing the nitridation reaction times from 1 h to 2.5 h (Fig. 1b–e), the diffraction peak intensities of AlN phase were increased significantly, which indicated that AlN particles were in situ formed in the AZ91alloys, and the amount of AlN particles was also gradually increased. Especially, when the nitridation reaction time was increased to 2.5 h, the diffraction peak intensities of $Mg_{17}Al_{12}$ phase were more weak, i.e. the amount of $Mg_{17}Al_{12}$ phase was significantly decreased, which has also been confirmed in the previous works, i.e. the in-situ formation of more AlN particles will lead to Al elements decreasing in the AZ91 matrix alloy melt, then less $Mg_{17}Al_{12}$ phases can be formed in subsequent solidification process [11–13].

Table 1
The chemical composition of the matrix alloy (AZ91, wt %).

Al	Zn	Mn	Si	Fe	Cu	Ni	Mg
9.13	0.74	0.27	0.04	0.001	0.001	0.0006	balance

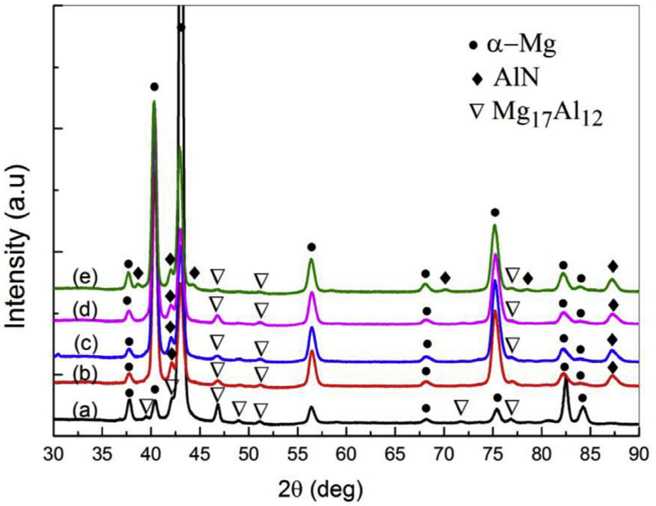

Fig. 1. XRD patterns of in-situ AlN/AZ91 composites with different nitridation reaction times: (a) 0 h; (b) 1 h; (c) 1.5 h; (d) 2 h; (e) 2.5 h.

Fig. 2 is the microstructural evolutions of in-situ AlN/AZ91 composites with nitridation reaction time increasing. When no AlN particles were in situ formed, i.e., the nitridation reaction time is 0 h (Fig. 2a), the primary α-Mg phase shows a typical dendritic structure in the as-cast AZ91 matrix alloy. With increasing nitridation reaction times, the shapes of primary α-Mg phase changed gradually from a typical dendritic structure to a cellular dendritic structure (Fig. 2b–d) and then to a similar equiaxial structure (Fig. 2e), which are also in agreement with the microstructure evolutions of primary α-Mg phase shape changing from a dendritic to a cellular structure due to Al element decrease in Mg-Al alloys [14]. In Fig. 2, it is also evident that the dendritic refinements were realized due to the in-situ formation of AlN particles. On the one hand, as heterogeneous nucleation sites of the primary α-Mg phase, firstly formed AlN particles improved nucleation rate due to a similar crystal lattice structure of AlN with α-Mg phases. On the other hand, the decrease of Al elements in residual liquid phase restrained the growth of α-Mg dendritic and eutectic structures (α-Mg and β-$Mg_{17}Al_{12}$ phases). Thus with increasing the nitridation reaction times, i.e. increasing the amount of AlN particles, the microstructure of matrix alloy was significantly refined.

In addition, from Fig. 3a, it is also obvious that β-$Mg_{17}Al_{12}$ phase exhibits a typical partially divorced eutectic morphology, i.e. the divorced eutectic β-$Mg_{17}Al_{12}$ phases with an interconnected reticulum were mainly located on the grain boundaries of primary α-Mg grains when no AlN particles were in situ formed. Once the nitridation reaction time was increased to 1 h, more granular eutectic β-$Mg_{17}Al_{12}$ phases started to form (Figs. 2b and 3b). Then, the interconnected reticulum β-$Mg_{17}Al_{12}$ eutectic phases were transformed completely into the dispersed granular structure in Fig.3b–e,

Download English Version:

https://daneshyari.com/en/article/11015835

Download Persian Version:

https://daneshyari.com/article/11015835

Daneshyari.com